Journal Pre-proof

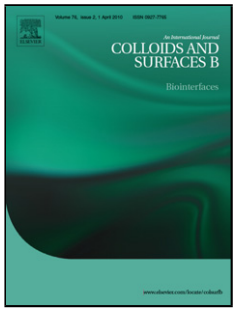

Development and characterization of an improved formulation of cholesteryl oleate-loaded cationic solid-lipid nanoparticles as an efficient non-viral gene delivery system

María J. Limeres, Marc Suñé-Pou, Silvia Prieto-Sánchez, Cristina Moreno-Castro, Alejandro D. Nusblat, Cristina Hernández-Munain, Guillermo R. Castro, Carlos Suñé, Josep M. Suñé-Negre, María L. Cuestas

PII: S0927-7765(19)30677-0

DOI: https://doi.org/10.1016/j.colsurfb.2019.110533

Reference: COLSUB 110533

To appear in: *Colloids and Surfaces B: Biointerfaces*

Received Date: 28 May 2019

Revised Date: 24 September 2019

Accepted Date: 26 September 2019

Please cite this article as: Limeres MJ, Suñé-Pou M, Prieto-Sánchez S, Moreno-Castro C, Nusblat AD, Hernández-Munain C, Castro GR, Suñé C, Suñé-Negre JM, Cuestas ML, Development and characterization of an improved formulation of cholesteryl oleate-loaded cationic solid-lipid nanoparticles as an efficient non-viral gene delivery system, *Colloids and Surfaces B: Biointerfaces* (2019), doi: https://doi.org/10.1016/j.colsurfb.2019.110533

Development and characterization of an improved formulation of cholesteryl oleate-loaded cationic solid-lipid nanoparticles as an efficient non-viral gene delivery system

María J. Limeres[a-c], Marc Suñé-Pou[*a,b], Silvia Prieto-Sánchez[b], Cristina Moreno-Castro[b], Alejandro D. Nusblat[d], Cristina Hernández-Munain[e], Guillermo R. Castro[f], Carlos Suñé[b], Josep M. Suñé-Negre[a], María L. Cuestas[*,c]

[a]Service of Development of Medicines (SDM), Faculty of Pharmacy, University of Barcelona, Barcelona, Spain. [b]Department of Molecular Biology, Institute of Parasitology and Biomedicine "López-Neyra" (IPBLN-CSIC), Granada, Spain. [c]Institute of Research in Microbiology and Medical Parasitology (IMPaM), Faculty of Medicine, University of Buenos Aires-CONICET, Buenos Aires, Argentina. [d]Institute of Nanobiotechnology (NANOBIOTEC), Faculty of Pharmacy and Biochemistry, University of Buenos Aires-CONICET, Buenos Aires, Argentina. [e]Department of Cell Biology and Immunology, Institute of Parasitology and Biomedicine "López-Neyra" (IPBLN-CSIC), Granada, Spain. [f]Nanobiomaterials Lab, CINDEFI, School of Sciences, National University of La Plata-CONICET (CCT La Plata), Buenos Aires, Argentina.

[*]CORRESPONDING AUTHOR

Marc Suñé-Pou

Phone: +34 600 568 315

E-mail: msunepou@gmail.com

María Luján Cuestas

Phone: +54 11 5950 9500 2177

E-mail: marilucuestas@gmail.com

Graphical abstract

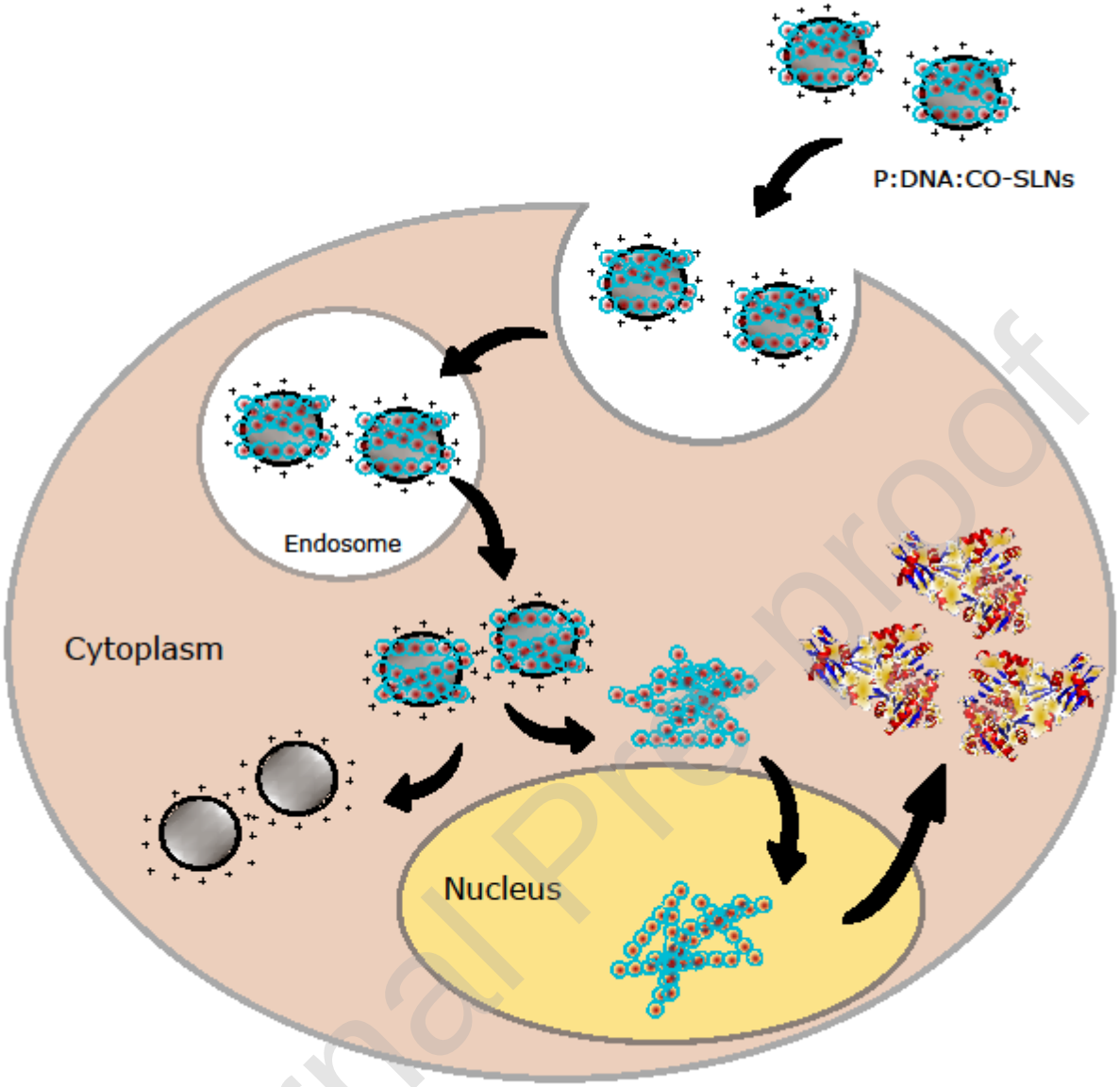

Highlights

- A CO-loaded cSLNs formulation was improved using protamine to enhance performance.
- The optimal P:DNA:CO-SLN ratio was 2:1:17 for the highest transfection activity.
- The obtained SLNplexes showed good particle size and zeta potential.
- Transfection efficiency of the P:DNA:CO-SLNplexes increased more than 200 times.
- *In vitro*, the P:DNA:CO-SLN plexes did not have a cytotoxic effect in human cells.

Abstract

Nanoparticle-mediated plasmid delivery is considered a useful tool to introduce foreign DNA into the cells for the purpose of DNA vaccination and/or gene therapy. Cationic solid-lipid nanoparticles (cSLNs) are considered one of the most promising non-viral vectors for nucleic acid delivery. Based on the idea that the optimization of the components is required to improve transfection efficiency, the present study aimed to formulate and characterize cholesteryl oleate-containing solid-lipid nanoparticles (CO-SLNs) incorporating protamine (P) to condense DNA to produce P:DNA:CO-SLN complexes as non-viral vectors for gene delivery with reduced cytotoxicity and high cellular uptake efficiency. For this purpose, CO-SLNs were used to prepare DNA complexes with and without protamine as DNA condenser and nuclear transfer enhancer. The main physicochemical characteristics, binding capabilities, cytotoxicity and cellular uptake of these novel CO-SLNs were analyzed.

Positively charged spherical P:DNA:CO-SLN complexes with a particle size ranging from 330.1 ± 14.8 nm to 347.0 ± 18.5 nm were obtained. Positive results were obtained in the DNase I protection assay with a protective effect of the genetic material and 100% loading efficiency was achieved at a P:DNA:CO-SLN ratio of 2:1:7. Transfection studies in human embryonic kidney (HEK293T) cells showed the versatility of adding protamine to efficiently transfect cells, widening the potential applications of CO-SLN-based vectors, since the incorporation of protamine induced almost a 200-fold increase in the transfection capacity of CO-SLNs without toxicity.

These results indicate that CO-SLNs with protamine are a safe and effective platform for non-viral nucleic acid delivery.

Key words: Cationic solid-lipid nanoparticles; plasmid DNA; protamine; cholesteryl oleate; transfection.

Introduction

Gene therapy and DNA vaccines attract attention in the medical, pharmaceutical and biotechnological fields due to their applications in the treatment of diseases for which there is currently no effective conventional therapy or for the induction of protective cell-mediated immunity against allergens, infectious agents or tumoral cells, for which there are no effective and safe licensed vaccines. In this regard, all currently licensed vaccines prepared from killed or inactivated whole cells, recombinant proteins or live attenuated microorganisms, stimulate the production of protective neutralizing antibodies. However, except for the vaccines prepared from live attenuated microorganisms, which raise concerns about their risks (virulence reversion), manufacturing process and transport, the others do not preferentially induce cellular immunity [1]. Hence, a novel approach to therapy and vaccination is the administration of nucleic acids that modulate the expression or suppression of certain proteins, thus reversing the disorder or genetic alteration or inducing protective cell-mediated immunity.

Despite the advances in this field, the application of plasmid DNA to treat human diseases with therapeutic or prophylactic purposes have been hampered by the poor clinical outcomes observed. Detrimental factors such as low cellular uptake, instability and rapid *in vivo* degradation by nucleases, unsatisfactory transport to the target and ineffective delivery of plasmid DNA to the cell nucleus [2] have prompted researchers to develop several strategies to overcome these barriers.

The development of an efficient carrier for gene-based medicines is thus considered a crucial factor for the successful application of genes in the treatment or prophylaxis of several human diseases. The limitations associated with the use of viral vectors, which are those related to safety problems (i.e., triggering of immune responses, failure in the insertion of the transgene, oncogenesis) and DNA package size limits [3,4] have encouraged the development of alternative methods for gene delivery. In this regard, nanotechnology has provided novel opportunities to improve the delivery of nucleic acids, using cationic molecules and structures such as polymers, lipids, peptides, nanoparticles, and lipid nanoemulsions as non-viral delivery systems [5]. All of them can bind nucleic acids and form complexes known as polyplexes or lipoplexes (depending on the nature of the cationic system) that can deliver genetic material to cells [6]. Among the advantageous features of these non-viral vectors are low toxicity, low immunogenicity, easy preparation, large-scale production, low-cost production, high-reproducibility and no DNA package size limits [7]. However, the transfection efficiency

is low during *in vivo* testing [8], underscoring the need for more effective nanocarrier formulations capable of high transfection efficiency without toxicity.

Cationic solid-lipid nanoparticles (cSLNs) are considered one of the most promising non-viral vectors for nucleic acid delivery. cSLNs are colloidal carriers consisting of oil-in-water microemulsions, in which the liquid lipid (oil) has been substituted by a solid lipid dispersed in water or in an aqueous surfactant solution [9]. cSLNs offer unique properties that make them especially attractive compared to other nanocarriers, such as small size, large surface area, the use of biocompatible excipients that minimize the risk of toxicity, the possibility of administering them by multiple routes (intramuscular, intravenous, nasal, ocular, oral, pulmonary, topical), the capability of transfecting DNA and RNA *in vitro* and *in vivo*, the existence of a safe and robust manufacturing process that allows efficient scaling for large-scale production, and the capability of sterilization by lyophilization [10-14].

Nevertheless, the main drawback of cSLN systems that could hinder their implementation for medical purposes is their tendency for polydispersity and aggregation during short- and medium-term storage [15]. The use of cholesteryl oleate (CO), a cholesterol derivative, in cSLN-nucleic acid formulations to improve cytotoxicity and transfection efficiency as a novel avenue for the development of highly efficient and biocompatible therapeutic carriers has been recently proposed [16]. In order to improve the capacity of CO-SLNs to transfect cells, protamine (P) has been previously incorporated to condense DNA and form lipoplexes on the nanoparticle surface [17].

Protamine is a small polycationic amine derived from the sperm of salmon, with MW~ 4,000–6,000 Da. Almost 67% of its amino acid composition is arginine, thus contributing to its high alkalinity [18]. Protamine is a positively charged nuclear protein that binds to the phosphate backbone of DNA using its arginine-rich domain as anchor. DNA is then stabilized and folded into a toroid, an O-shaped structure that may allow for dense DNA packaging, in a similar way to histones. Protamine is considered an attractive biopolymer in the field of pharmaceutical technology due to its biocompatibility and has been used in several marketed pharmaceutical products such as insulin for many years [19]. Protamine is also used as a pharmaceutical drug to neutralize heparin after surgery or for the treatment of heparin overdose [20]. Protamine also has cell-penetrating and nucleus-targeting properties and its sulfated salt has been shown to be a safer and more appropriate alternative to poly-L-lysine for condensation, as well as the delivery of plasmid DNA to the nucleus [21]. Furthermore, protamine salts have often been used in combination with liposomal preparations to deliver plasmid DNA into cells [22-24]. These ternary complexes were designed to mimic viral vectors

containing condensed DNA, which is surrounded by a lipid bilayer. The capacity of protamine to promote the transfection of retinal cells with cSLNs was also demonstrated [2,25]. The understanding of the mechanism by which protamine increases the transfection efficiency of cSLNs was elegantly shown by Delgado et al [25], and it was related to the presence of nuclear localization signals (NLS) in the protamine molecule, its protection capacity, and a shift in the internalization mechanism from caveolae/raft-mediated to clathrin-mediated endocytosis. Then, the *in vivo* usefulness of cSLNs to transfect ocular tissues was finally shown using vectors prepared with cSLNs and protamine demonstrating their potential application for the management or treatment of degenerative retinal disorders as well as ocular surface diseases, such as X-linked juvenile retinoschisis [26]. All these properties make protamine a very useful compound for transfection approaches.

Based on this premise, we designed novel cationic ternary nanoparticles for gene delivery, consisting of P/DNA complexes adsorbed on the cationic CO-SLN surface in an effort to expand our previous work and improve the transfection efficiency of CO-SLN without toxicity, for their future application on gene therapy or DNA vaccines.

Different complexes were prepared by modifying the P:DNA:CO-SLN mass ratios and transfection efficiency and cell uptake in human embryonic kidney (HEK293T) cell line were studied.

2. Materials and methods

2.1 Production of CO-SLNs

The CO-SLNs were manufactured using the hot microemulsion technique, as previously described [27]. The components of the lipid matrix (41.7% of the formulation) were stearic acid (EMD Millipore, Billerica, MA, USA) and cholesteryl oleate (Tokyo Chemical Industry Co., Tokyo, Japan), poloxamer 188 (8.3% of the formulation, from EMD Millipore) and the cationic lipid octadecylamine (50% of the formulation, from Acros Organics, Geel, Belgium) was used as charged carrier [16]. Briefly, the lipid matrix was melted at a temperature above its melting point while the hydrophilic components were separately heated in ultrapure water (EMD Millipore). Later, the components were mixed and stirred at the same temperature (80 °C) to form a hot emulsion. After stirring for 10 minutes, the microemulsion was dispersed into refrigerated water (4 °C) in continuous agitation to produce the core solidification of the cSLNs. The emulsion was centrifuged at 19,000 x *g* for 15 min and double filtered with 43-48 µm and 7-9 µm qualitative filter papers (FILTER-LAB®, Filtros ANOIA, S.A. Barcelona). The nanoparticle suspension was then mixed with a solution of the

cryoprotectant trehalose (5%, w/v) and freeze-dried to improve its stability and feasibility using a Lyobeta 20 (Telstar, Terrassa, Spain) pilot freeze-drying system.

Dye-labeled samples were prepared by adding 200 µl of a methanol solution of 2 mg/ml Nile Red (EMD Millipore) to the lipid matrix of SLN suspension before melting [28]. Nile Red is a fluorescent dye that interacts with lipids and allows them to be visualized without dissolving them [29].

All assays, except for the fluorescence microscopy studies, were performed using freeze-dried cSLNs re-dispersed in ultrapure water (3.0 ml).

2.2 Plasmid DNA constructs

The plasmid vector expressing the p3X-Kβ-L firefly luciferase protein has been previously described [30]. A dual luciferase assay kit (Promega, Ca, USA) was used for the detection of luciferase activity. For fluorescence microscopy experiments the pcDNA3.1 + N-eGFP plasmid vector was used (GenScript, Piscataway, USA).

2.3 Formation of lipoplexes

P:DNA:CO-SLN vectors were made using 1.0 mg/ml protamine sulfate (EMD Millipore.) mixed with 1000 ng of p3X-Kβ-L plasmid (0.75 mg/ml), at a ratio of 2:1 (w/w) for 5 min. Then, the P:DNA complex was mixed with a suspension of CO-SLNs at room temperature for 20 min, and electrostatic interactions between the P:DNA complexes and CO-SLNs led to the formation of P:DNA:CO-SLN vectors. After incubation, the vectors were diluted in Dulbecco´s Modified Eagle Medium (DMEM) low-glucose without penicillin/streptomycin or heat-inactivated fetal bovine serum (FBSi) for the transfection experiments. Different DNA masses were tested, *i.e*. 250 ng, 500 ng, 750 ng and 1000 ng respectively. As control, DNA:CO-SLN vectors were prepared by mixing an aqueous solution of the p3X-Kβ-L plasmid (0.75 mg/ml) together with 7.0 µl of the CO-SLN suspension (72 µg/µl) at room temperature for 20 min to allow the complex to be formed. After incubation, the DNA:CO-SLN complexes were diluted in DMEM low-glucose without antibiotics or FBSi. In all cases, different DNA masses were tested, as stated before.

2.4. Determination of particle size and surface charge (zeta-potential)

Analyses of CO-SLN sizes were determined by laser diffraction on a Mastersizer 2000 (Malvern Instruments, UK) equipped with a 4 mW He–Ne laser (633 nm). For DNA:CO-SLNs and P:DNA:CO-SLN complexes, sizes and polydispersity index (PDI) were measured by dynamic light scattering on a Zetasizer Nano ZS90 (Malvern Instruments).

The zeta potential of all formulations was measured by laser Doppler microelectrophoresis in a Zetasizer Nano-Z (Malvern Instruments, UK). The zeta-potential values were obtained from the electrophoretic mobility of the nanoparticles and lipoplexes under an electric field. Measurements were made in triplicate and expressed as millivolts (mV).

2.5. Morphological analysis by transmission electron microscopy (TEM)

The surface and content homogeneity of the nanoparticles and lipoplexes was analyzed using TEM. Images were acquired from reconstituted CO-SLNs after freeze-drying in the presence of trehalose 5% (w/v) using a Tecnai Spirit microscope equipped with a LaB6 cathode (FEI Company, Hillsboro, OR, USA). Images were recorded at 120 kV using a 1376 x 1024 pixel CCD Megaview camera. The samples were adsorbed onto carbon-coated copper grids and were negatively stained with a 2.0% uranyl acetate solution.

2.6. Differential scanning calorimetry (DSC)

The possible interactions of the components in the formulation were assessed using DSC, as previously described [31]. Briefly, DSC was performed in a DSC-822e (Mettler Toledo) at a heating rate of 10 °C/min over a range from 30 °C to 200 °C using the heat flow method. The samples were weighed into a 40 µl aluminum pan, and an empty pan was used as a reference. Dry nitrogen (50 ml/min) was used to perform the assay in a nonoxidative atmosphere.

2.7. Electrophoresis on agarose gel

Loading efficiency of CO-SLNs with and without P and different DNA masses, as well as protection from DNAse I digestion (Roche Diagnostics GmbH, Mannheim, Germany) and DNA plasmid release from the vectors were carried out using a 1.0% agarose D-1 gel containing 0.04 µl/ml RedSafe® for nucleic acid visualization at 80 V for 45 min. The samples were visualized in a GelDoc® EZ Imager (BioRad®, USA) system using BioRad® ImageLab 5.2.1 software.

For the DNase I protection assay, complexes were prepared to a final mass of 1000 ng of DNA. A concentration of 1 U DNase I/2.5 µg DNA was added to DNA:CO-SLN and P:DNA:CO-SLN vectors, and the corresponding mixtures were then incubated at 37°C for 10 min. After incubation, a solution of 0.2 M EDTA (pH 8.0) was added to a final concentration of 8 mM and heated to stop the reaction at 75°C for 4 min. Then, 10% SDS was added to the samples to a final concentration of 1.0% to release the DNA from the CO-SLN lipoplexes. Finally, the integrity of the DNA in each sample was compared to an untreated DNA control.

2.8. Cell culture

HEK293T cells (human embryonic kidney 293T cells) were obtained from the American Type Culture Collection (ATCC, Manassas, VA, USA). The cells were grown and maintained in DMEM medium with low glucose supplemented with 10% v/v of heat-inactivated FBS (Life Technologies Corp., Eugene, OR, USA), penicillin/streptomycin, 4 mM L-glutamine and non-essential amino acids, at 37°C in a 95% air and 5% CO_2 atmosphere as previously described [27].

For all the biological assays implicating nucleic acids, the complexes were prepared by mixing CO-SLNs with the appropriate amount of DNA or P:DNA, as mentioned in the above sections.

2.9. Cell viability and proliferation assays

For the viability/cytotoxicity assays, HEK293T cells were grown in 35 mm plates (Falcon Enamelware, London, UK) to approximately 60%–70% confluence. After 48 h of incubation with complexes, cells were harvested and processed for cytotoxicity of the different lipoplexes using the propidium iodide (PI) test [32]. Briefly, HEK293T cells were seeded in 6-well plates (2.5 $x10^5$ cells/well) and incubated in DMEM supplemented with 10% FBSi at 37°C for 24 h. The culture medium was removed and the nanoparticles and lipoplexes were added in DMEM without antibiotics or FBSi and cells were incubated again at 37°C for 48 h. Flow cytofluorometric analyses were performed with the vital dye PI (40 µg/ml, EMD Millipore) using a FACSCalibur cytometer (BD Biosciences, San Jose, CA, USA). A minimum of 10,000 events was acquired gating the forward and side scatters to exclude cell debris and analyzed in FL-3.

The proliferation assay was determined in 96-well plates using the 3-(4,5-dimethylthiazol-2-yl)-2,5-diphenyltetrazolium bromide (MTT) assay after 24, 48 and 72 h of incubation (Roche, Mannheim, Germany). The absorbance at λ= 570 nm was determined using an enzyme-linked immunosorbent assay (ELISA) reader.

2.10. In vitro transfection assay

The transfection efficiency of the vectors was studied in HEK293T cells grown in 6-well plates by seeding the cells at 2.5 $x10^5$ cells/well and cultured for 24 h as described above. When cells reached approximately 60-70% of confluence, the medium was changed to a medium without serum or antibiotics.

The mixture CO-SLN/DNA and CO-SLN/P:DNA was kept at room temperature for 20 min to allow the complexes to form before transfection. Lipoplexes were prepared by mixing 1000 ng of the p3X-Kβ-L plasmid, and the amounts of CO-SLNs derived from the viability assay as mentioned earlier. The mixtures were added to the cells, and after 4–6 h, 200 µl of serum was added to each well. The cells were harvested approximately

48 h after transfection and processed for luciferase activity using the Dual-Luciferase® Reporter Assay (Promega Corporation, Madison, WI, USA) protocol following the manufacturer's instructions.

Different DNA:CO-SLNs and P:DNA:CO-SLNs w/v and w/w/v ratios respectively were tested (250:7; 500:7; 750:7, 1000:7 and 500:250:7; 1000:500:7; 1500:750:7; 2000:1000:7).

Cells transfected with P:DNA at 2:1 w/w ratio were used as control following an identical procedure. P:DNA:CO-SLN lipoplexes with a non-coding plasmid for the luciferase enzyme were used as negative control. At the end of incubation, cells were collected and lysed with a T7 buffer containing PMSF and DTT at 4°C for 30 minutes. After centrifugation at 16,000 x *g* the supernatant was recovered to measure the activity of luciferase.

2.11. Cellular uptake of non-viral vectors

The uptake of vectors by HEK293T cells was studied by fluorescence microscopy using an Olympus wide-field microscope and Cell-R IX81 software. For this purpose, CO-SLNs were labelled using the fluorescent dye Nile Red (absorption= 553 nm) and the process continued as described in the *in vitro* transfection assay. Cells were fixed with 3.5% PFA at 4°C for 45 minutes and protected from light after incubation with the complexes for 1 h and 24 h. Later, the cells were washed three times with PBS and permeabilized with 0.5% Triton X-100 at RT for 5 minutes. Then the cells were washed another three times with PBS and the nuclei were stained with DAPI (blue). After two more washes with PBS, preparations were finally mounted with ProLong® Gold antifade reagent (Life Technologies Corp.). Plasmid coding for the GFP protein (pcDNA3.1 + N-eGFP plasmid) was used to demonstrate the transfection capability of the lipoplexes. Non-Nile Red labeled CO-SLNs were used as negative control. Images were converted to a compatible format to deconvolve using the Imaris 4.0 software (Bitplane) and then were deconvolved with Huygens Essential software 3.4 version. All images were analyzed using Fiji/ImageJ software 1.52i version.

2.12. Statistical analyses

Statistical analyses were performed using Prism 5.0 software (GraphPad). Two-tailed Student's tests (unpaired t-test) were used to compare the samples and their respective controls. The P values are represented by asterisks (*: $P< 0.05$; **: $P< 0.01$; and ***: $P< 0.001$). The absence of an asterisk indicates that the change relative to the control is not statistically significant.

3. Results

3.1 Size and zeta potential of CO-SLN and DNA complexes

Particle size ranged from 330.1 ± 14.8 nm to 347.0 ± 18.5 nm and from 856.8 ± 242.6 nm to 1029.9 ± 212.2 nm in those SLNplexes obtained with and without P, respectively. The PDI was always higher than 0.4 in those SLNplexes obtained without P.

With regard to zeta potential, complexes showed a positive surface (+38.5 ± 1.1 mV for P-containing SLNplexes, and +23.2 ± 1.2 mV for non-P-containing SLNplexes).

The CO-SLNs were manufactured using the hot microemulsion technique which allows to obtain small and homogeneous nanoparticles around 180 nm. Due to the instability of the fresh prepared SLN suspensions, the reconstituted lyophilized CO-SLN powder was used in all the assays. Nevertheless, after the freeze-drying process, the same size and positive charge were observed (187 ± 18 nm and +33.3 ± 0.5 mV, respectively).

The SLNplexes sizes varied according to the DNA masses and P:DNA proportion (Figures 1A and B). In general, sizes were significantly higher ($P< 0.01$) for the vectors prepared without P than for the P:DNA:CO-SLN vectors (around 4 times).

Vectors without P showed similar size patterns, and became smaller as the DNA quantity increased from 250 to 1000 ng; however, their sizes remained too large to transfect cells efficiently [28].

In the case of SLNplexes with P, their sizes did not change considerably/significantly when the DNA quantity increased from 250 to 1000 ng (percentages varied from 6.5% to 0.5%). However, 1000 ng of DNA was used to achieve an efficient transfection. Size differences in SLNplexes related to the different proportions of P:DNA tested were not observed. Nevertheless, we proposed a 2:1 ratio as the ideal one because an excess of P might hinder DNA delivery within the cell nucleus.

Figure 1A. Size of complexes according to different DNA masses tested from 250 to 1000 ng.

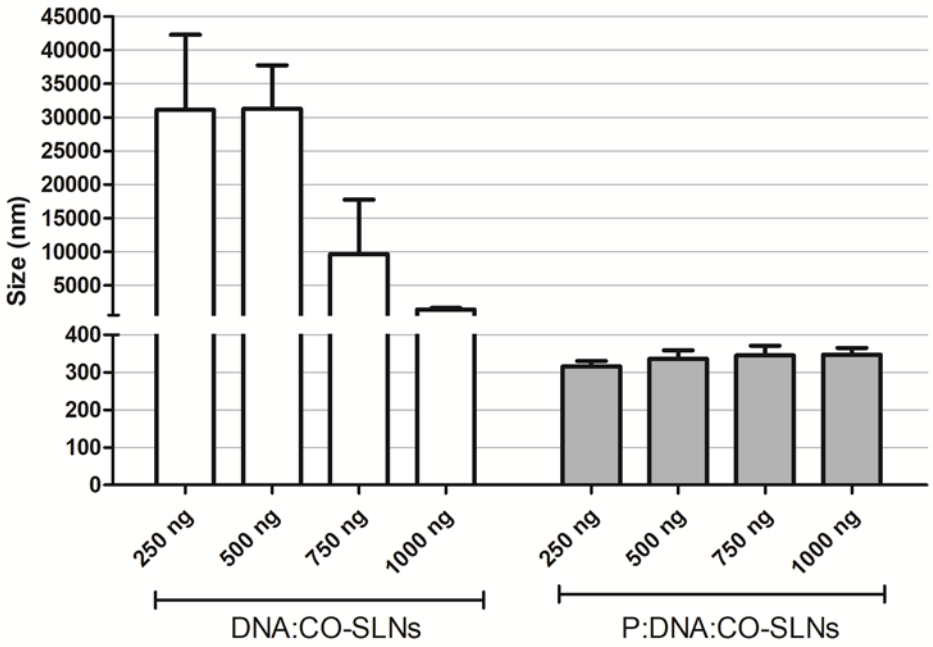

Figure 1B. Size of complexes according to different P:DNA proportions. In all cases, the same DNA mass and amount of CO-SLNs were used.

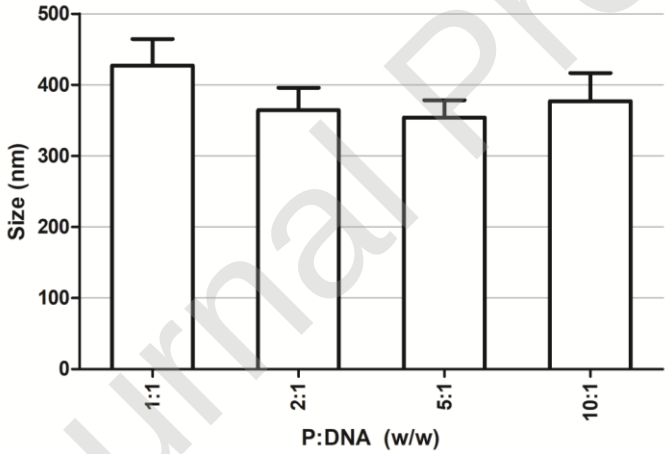

The TEM images confirmed the results obtained with the Mastersizer (Figure 2). The CO-SLNs showed spherical morphology and homogenous surfaces with particle sizes consistent with those determined previously. No aggregates were observed, supporting the stability of the resuspended freeze-dried particles. Similarly, P:DNA:CO-SLNs showed spherical morphology with particle sizes larger than their counterpart without P:DNA and a monodisperse distribution. In contrast, the TEM images of DNA:CO-SLN lipoplexes showed fusion of the CO-SLNs after binding to the DNA, resulting in lipid–DNA particles with undefined morphology, high polydispersity index and sizes between 600 and 1200 nm.

The compatibility among the components in the formulation was assessed using DSC. The results indicate that there are no interactions among cholesteryl oleate, stearic acid, octadecylamine, poloxamer 188 and protamine. Mixtures between the components exhibited no exothermic peak, which indicates that there are no physical or chemical interactions and thus validates this formulation for further studies (Supplemental file 1).

Figure 2. Morphological analysis of CO-SLN **(A)**, DNA:CO-SLN **(B)** and P:DNA:CO-SLN **(C** and **D)** complexes by transmission electron microscopy.

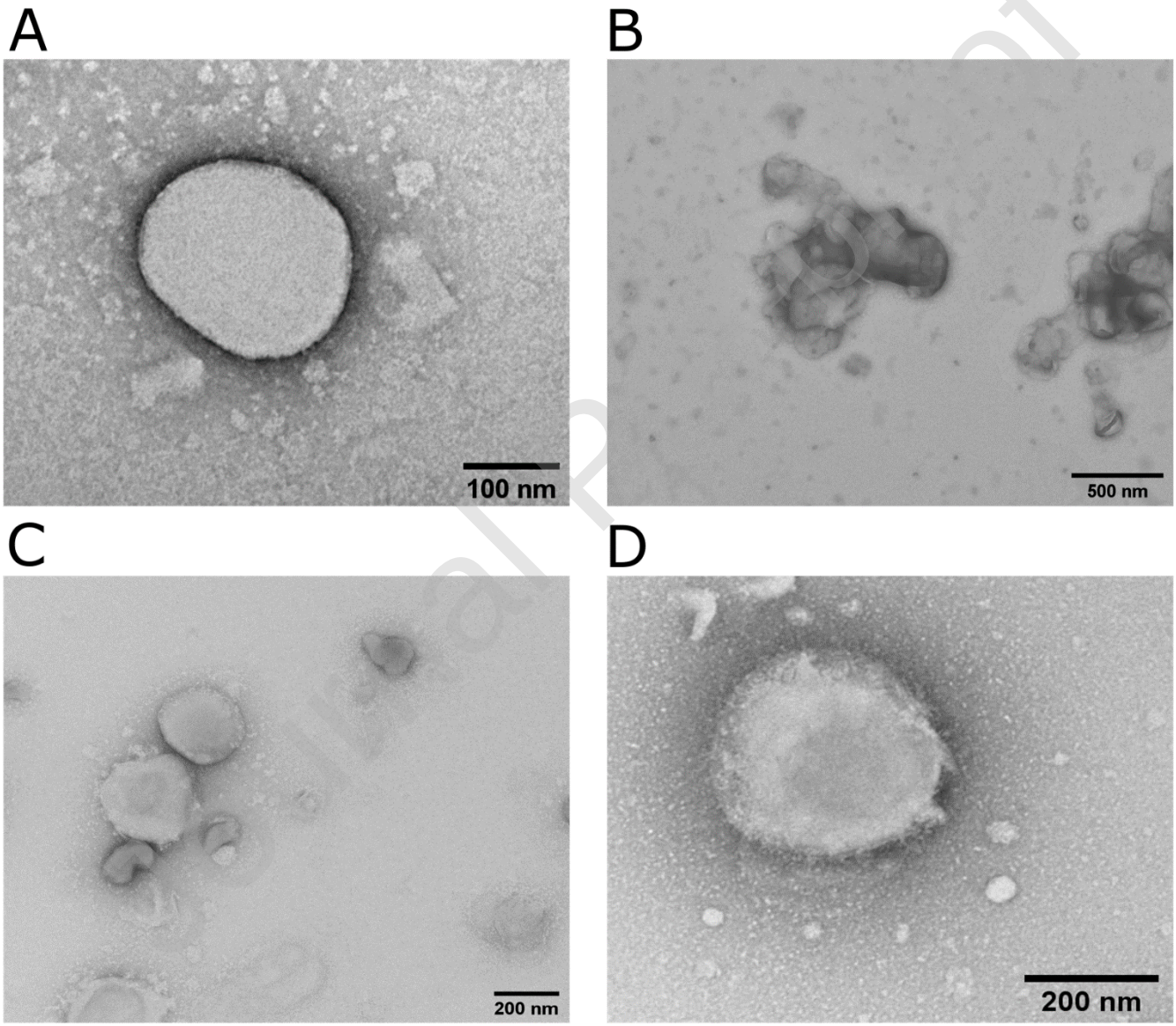

3.2. Determination of binding efficiency

The DNA plasmid was partially bound in those vectors without P at DNA masses higher than 2 µg (Figure 3A), whereas the DNA plasmid was fully bound in all the vectors containing P (Figure 3B). The protection capacity of the vectors and their release of DNA were analyzed by the integrity of DNA in agarose gel electrophoresis after treatment with DNase I and SDS, respectively.

Figure 3. Loading efficiency of cSLN (A) and complexes with P (B) at different amounts of plasmid DNA by agarose gel electrophoresis. Lanes 1 to 5: DNA only from 1000, 1500, 2000, 2500 and 3000 ng (A B). Lanes 6 to 10: DNA:CO-SLN complexes with a fixed amount of 7 µl of CO-SLNs and an increasing amount of DNA from 1000, 1500, 2000, 2500 and 3000 ng (A). Lanes 6 to 10: P:DNA:CO-SLN complexes with a fixed amount of 7 µl of CO-SLNs and a P:DNA w/w ratio of 2:1 from 1000, 1500, 2000, 2500 and 3000 ng of DNA (B). Molecular weight marker: 10, 8, 6, 5, 4, 3, 2 and 1.5 kb.

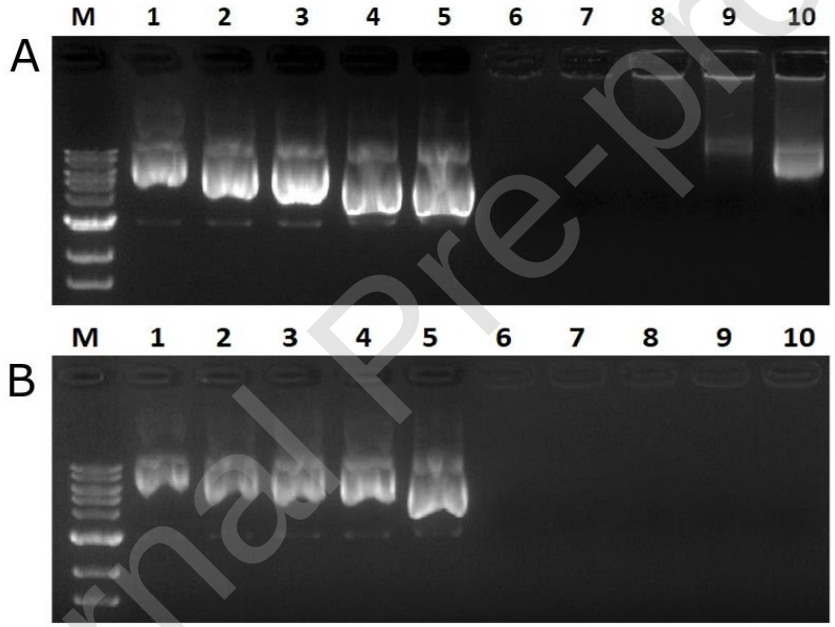

The formulations assayed preserved the integrity of the transported DNA (Figure 4), although the band corresponding to the supercoiled DNA topoisoform (lower band, which is the most bioactive isoform) was more intense in the vectors containing P after treatment with DNase I and SDS. Moreover, all vectors treated with SDS were able to release DNA.

Figure 4. Protection of DNA from DNase I by DNA:CO-SLN and P:DNA:CO-SLN complexes at ratios (w/v and w/w/v) of 1:7 and 2:1:7, respectively, visualized by agarose gel electrophoresis. Lane M: MW marker: 10, 8, 6, 5, 4, 3, 2 and 1.5 kb. Lane 1: free DNA; Lane 2: free DNA treated with DNase I; Lane 3: DNA:CO-

SLNs (1:7); Lane 4: P:DNA:CO-SLNs (2:1:7); Lane 5: DNA released from DNA:CO-SLN complexes with SDS 1%; Lane 6: DNA released from P:DNA:CO-SLN complexes with SDS 1%; Lane 7: DNA:CO-SLNs treated with DNase I and SDS 1%; Lane 8: P:DNA:CO-SLNs treated with DNase I and SDS 1%. Different forms of DNA: Open circular (OC), Linear (L) and supercoiled (SC).

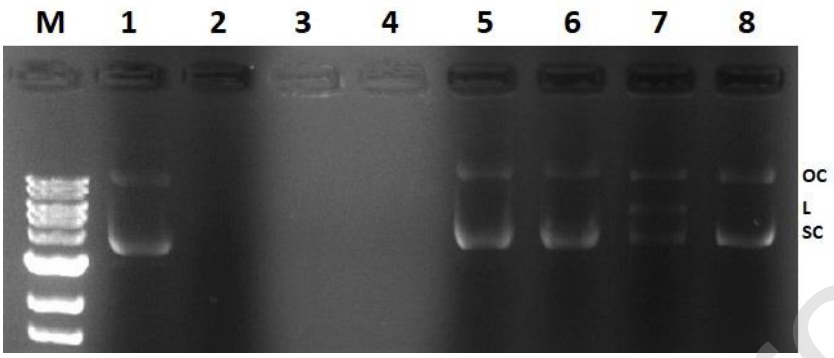

3.3. Cell viability

The cell viability/cytotoxicity of the CO-SLN vectors and their corresponding SLNplexes with and without P was studied on HEK293T cells. As shown in Figure 5A, no toxic effect of all these vectors and SLNplexes were observed by the IP test. These results thus suggest that the CO-SLN SLNplexes are not harmful to human cells cultured *in vitro* under the performed experimental conditions. The cytotoxicity against HEK293T cells was also studied using the MTT colorimetric cell proliferation assay. While initial low proliferation was observed at 48 h after treatment, the cells recovered quickly and showed almost normal viability at a later treatment time point (72 h). As it is shown in Figure 5B no significant differences in the cell proliferation were observed in those cells exposed during 24h, 48 h and 72 h with the SLNplexes.

Figure 5. (A) Cell viability of HEK293T cells after 48 h of CO-SLN and lipoplex exposure by flow cytometer. **(B)** Proliferation assay in HEK293T at different times (24 h, 48 h and 72 h) after transfection with DNA:CO-SLN and P:DNA:CO-SLN complexes.

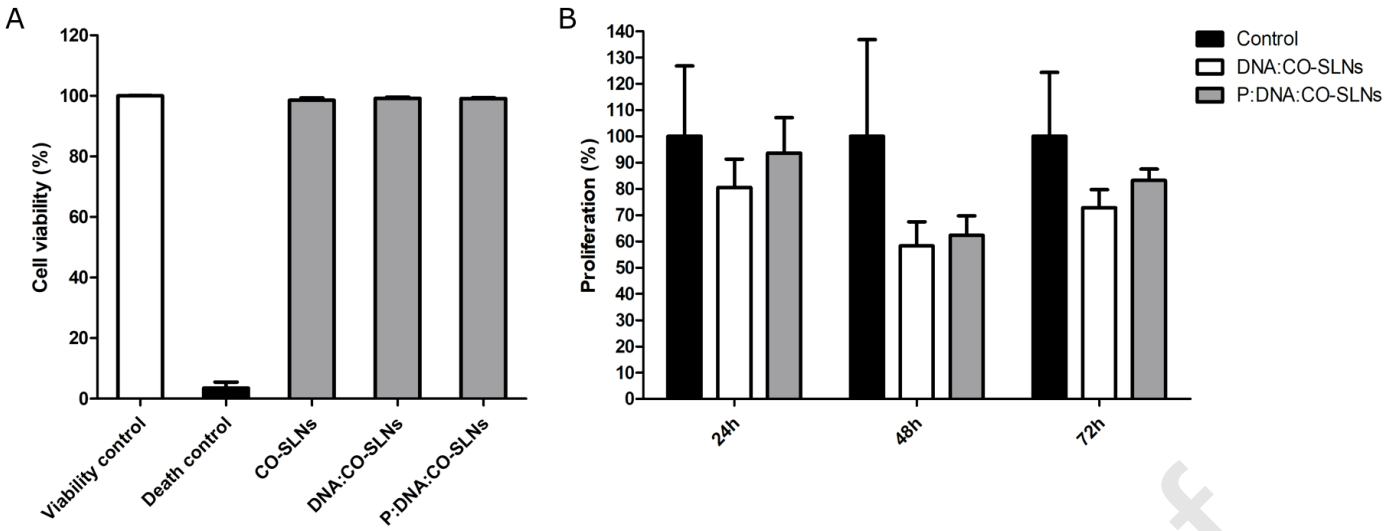

3.4. Cellular uptake and biological activity

The cellular uptake of SLNplexes and their capability to generate a biological response were tested by the luciferase reporter assay, where pDNA driving the expression of the luciferase gene was transfected into HEK293T cells. A dose–response effect in the luciferase activity was observed upon transfection with different DNA:CO-SLN and P:DNA:CO-SLN mass ratios. As shown in Figure 6A and 6B, the enzymatic activity increased upon transfection with higher amounts of DNA, and the formulations containing P induced almost a 200-fold increase in the transfection capacity of the CO-SLNs vectors.

The cellular uptake and localization of the Nile Red-labeled SLNplexes was evaluated by fluorescence microscopy after 1 h and 24 h of transfection of HEK293T cells (Figure 7A and 7B respectively). Numerous and diffuse red fluorescent dots were observed in the cytoplasm after 1 h of transfection with the P:DNA:CO-SLNs, indicating a rapid interaction of the complexes with the cells. Unlike the P-containing CO-SLN SLNplexes that showed a homogeneous fluorescent pattern, the red fluorescent signal from the SLNplexes not containing P was less homogeneous and with numerous aggregates, supporting the results obtained with the different particle sizes of lipoplexes. At 24 h post-transfection, a weak red fluorescent signal was observed in the complexes containing and not containing P, indicating their cellular uptake and degradation. In both transfection systems we could visualize the expression of GFP and hence the ability of both SLNplexes to generate a biological response as was assessed in the luciferase reporter assay.

Figure 6. Comparison between transfection efficiency of DNA:CO-SLNs vs P:DNA:CO-SLNs in HEK293T cells by the luciferase reporter assay. After 24 h of confluence, cells were transfected with both systems and harvested at 24 h post-transfection to be analyzed **(A B)**. DNA mass was tested from 250 to 1000 ng **(A)**. The DNA:CO-SLNs and P:DNA:CO-SLN mass ratio correspond to 1:7 and 2:1:7 respectively **(B)**. Three independent experiments were performed in triplicate. ****P*< 0.001.

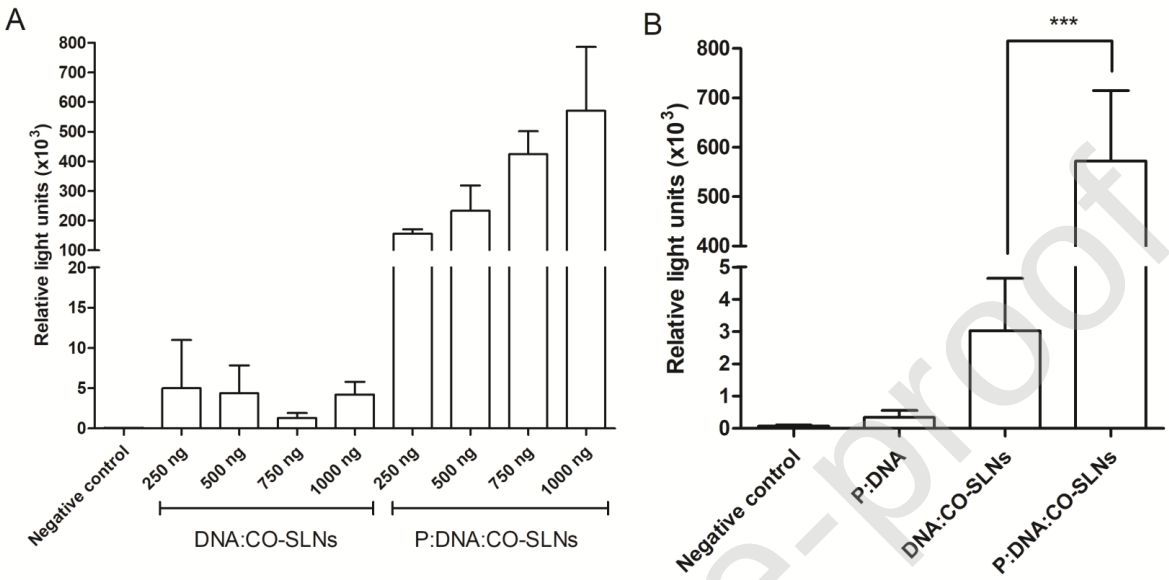

Figure 7. Fluorescence microscopy images of HEK293T cells transfected with Nile Red-labeled (red) DNA:CO-SLN and P:DNA:CO-SLN complexes at 1 h **(A)** and 24 h **(B)** after transfection. HEK293T cells were treated with DAPI (blue) and the DNA plasmid used corresponds to pcDNA3.1 + N-eGFP. The gray images correspond to the respective transmitted light to each condition to visualize the extension of the cytoplasm.

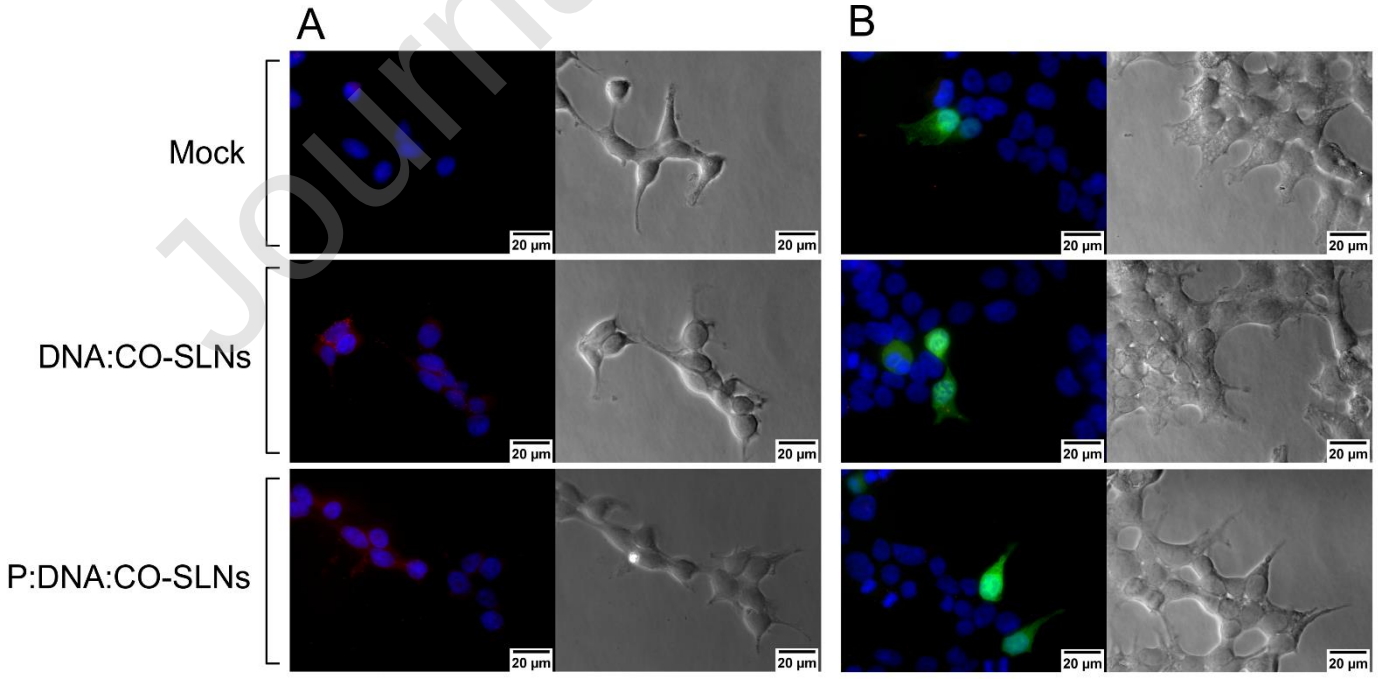

Discussion

The use of the cholesterol derivative CO as a novel excipient for SLN formulations for the development of highly efficient and non-toxic nucleic acid delivery carriers has been previously reported [15,16,27].

The incorporation of NLS into non-viral vectors was studied by several authors, and it has been shown to improve transfection efficiency due to an effect on the nuclear membrane [33-35]. Protamine, a peptide widely used to improve lipofection due to its rich content in NLS, is expected to produce an enhancement of the transfection efficacy of CO-SLNs associated to their nuclear localization and stabilization against DNase degradation [36].

Therefore, in the present study, the use of protamine was proposed to obtain an improved formula that maintains the nanoparticle structure, morphology and nucleic acid binding efficiency while improving both viability and transfection efficiency to induce potent biological activity.

In the present study, a simple fabrication method with inexpensive reagents, which allows a simple procedure for potential scale-up production of SLNs was used.

According to Faneca et al [37], DNA condensation is necessary to facilitate the mobility of DNA molecules as well as to prevent them from inter- and intra-cellular degradation. Nevertheless, the transfection efficiency of non-viral systems could be limited by the degree of DNA condensation [38]. Thus, the influence of P:DNA:CO-SLN mass ratios on the transfection efficiency and cell uptake in HEK293T cell line was also studied to evaluate the role of P as an important factor to improve formulation, and thus its further application in gene therapy and/or DNA vaccination.

SLNplexes containing P showed smaller sizes in comparison with those not containing P in all the pDNA:SLN ratios tested. Moreover, P lipoplexes showed mean diameters less than 500-700 nm by far below the size of DNA:CO-SLNs, which are larger than 1 µm. This size should be suitable for uptake by endocytic processes or direct fusion within the cell membrane [39,40]. In fact, cellular uptake could be shown by fluorescence microscopy and resulted in the expression of the encoded reporter gene in at least some cells as discussed below.

TEM images of the SLNplexes without P suggested fusion of the CO-SLNs after binding to the DNA, resulting in irregular lipid–DNA particles with sizes between 600 and 1200 nm.

With regard to zeta potential, complexes showed a positive surface. This value was about +38.5 ± 1.1 mV for P-containing SLNplexes, and +23.2 ± 1.2 mV for non-P-containing SLNplexes. It is generally considered that nanoparticles displaying Z-potential outside the range of ± 25 mV have high stability degrees.

The more positive Z-potential with P-containing SLNplexes provides evidence that the negative charges of DNA were almost completely redressed, whereas a less positive charge obtained in the non-P-containing SLNplexes indicate partial DNA complexation, results that were also confirmed in the gel electrophoresis retardation assays. Thus, the addition of P to form DNA:CO-SLN SLNplexes demonstrated an excellent property to promote pDNA condensation, being able to form small complexes, while non-P-containing SLNplexes formed large aggregates of DNA:CO-SLNs. In the case of P:DNA:CO-SLNs, the images obtained by TEM showed, spherical nanoparticles with homogeneous surfaces, whose sizes were consistent with those measured on a Zetasizer Nano ZS90 (below 350 nm in an average diameter), whereas P-free complexes exhibited irregular shapes and a variety of sizes that explain the high PDI values determined by DLS.

Overall results thus showed that vectors prepared without P showed a bigger size, higher PDI and lower zeta potential than vectors prepared with P.

A slightly positive zeta potential of SLNplexes is advantageous because it facilitates the interaction with the negatively charged cell surface and the cell entry; high positive charges are unfavorable because of severe cytotoxic effects [28,41]. In agreement to a previous report using CO-SLNs [31], all the excipients used in the present formulation of the cSLNs showed no interactions among the components and, consequently, revealed a good compatibility.

The nucleic acid binding efficiency to the CO-SLNs with and without protamine was assessed using agarose gel electrophoresis. The presence of unbound free DNA in the gels reflects the binding capacity of the nanoparticles. In the absence of P, when the DNA amount was 1.0-2.0 µg, no free DNA was observed in the gel, which indicated that the DNA was completely bound to the CO-SLNs. When 2.5 µg of DNA was used, minimal free DNA was observed in the gel, and considerable free DNA was detected in the gel upon loading 3 µg of DNA. However, when P was added to form the DNA complexes, the DNA was completely bound to the CO-SLNs at all DNA concentrations assayed, demonstrating the versatility of P to condense the DNA and improving complexation with CO-SLNs. These results confirmed the suitability of CO-SLNs for DNA binding observed in previous works [15,16,27] and the enhancement of the binding efficiency by adding P to DNA molecules prior to SLNplex formation with CO-SLN. Furthermore, the capacity to protect DNA from the

components of the medium, especially from DNase digestion, is considered an important advantage of non-viral systems used for the delivery of nucleic acids [42]. In order to study the protection capacity of the novel SLNplexes with P, we exposed the DNA:CO-SLN and P:DNA:CO-SLN complexes to DNase I at 37°C for 10 min, and the integrity of the DNA was analyzed by gel electrophoresis. The results demonstrated that all the formulations assayed were able to preserve DNA integrity, although the intensity of the band corresponding to the supercoiled DNA topoisoform increased in the vectors containing P, indicating that the protection of DNA from DNases can be correlated with the degree of nucleic acid condensation. Moreover, all SLN vectors treated with SDS were able to release DNA, which is one of the most crucial steps to achieve an optimal CO-SLNs-mediated transfection assay suggesting that the degree of condensation obtained with P is not excessive enough to limit transfection in *in vitro* assays. Another important aspect to be considered is DNA topology, and supercoiled DNA has been reported in the literature to be the most bioactive form, with the highest transfection capacity [43]. Interestingly, it was reported that the presence of the linear form of DNA topology after treatment with DNAse I observed in the SLNplexes without P is the result of cutting one of the DNA double strands of the supercoiled-DNA by DNase I, turning this DNA topology into open circular DNA, which in a successive cut, breaks this isoform to the linear one [44]. Thus, the formulations containing P are the ones that better protect DNA from DNase I, and thus, the P-formulation should be the most convenient for transfection from a DNA topology point of view.

Bearing these results in mind, cell viability and transfection efficiency were evaluated in order to understand how the different CO-SLN SLNplexes using different DNA condensation capacities with or without P influenced their *in vitro* behavior. As size and Z-potential values of these SLNplexes suggested that they might be considered suitable for DNA delivery, these non-viral carriers were applied in the transfection and fluorescence experiments. In all cases, the percentage of live cells, determined by flow cytometry was close to 100% for both the cells treated and not treated with SLNplexes, indicating that these SLNplexes are non-cytotoxic to human cells under the experimental conditions.

The ability of the SLNplexes formulated herein to deliver DNA into cells and generate a biological response was assessed analyzing the transfection capacity of the CO-SLNs using the p3X-Kβ-L plasmid that codes for the firefly luciferase, as reporter system. In order to support these results, fluorescence microscopy was used to assess the transfection capacity and the cellular uptake and localization of the SLNplexes. Large and few red fluorescent dots were observed in the cytoplasm and in the nucleus after transfection with the pcDNA3.1 + N-eGFP plasmid with all the Nile Red-labeled CO-SLN SLNplexes after 24 h, supporting the

results obtained with the luciferase reporter assay suggesting that CO-SLNs with and without P can be internalized in cells and generate a biological response, GFP expression. Unlike the CO-SLN SLNplexes without P that showed numerous aggregates at 1h post-transfection, the red fluorescent signal from the P-containing SLNplexes was clear and homogeneous. These observations suggest that the P:DNA:CO-SLN complexes have a surface that provides cell binding and intracellular uptake. The presence of NLS sequences with high arginine content in the protamine molecule is associated to an enhanced DNA entry into the nucleus [45,46]. Therefore, these vectors provided protection against nuclease activity, enabling cellular uptake, intracellular nucleic acid release and RNA transcription in the nucleus, transport to the cytoplasm, and translation into protein, enabling bioactivity. The addition of P to the CO-SLN formulation showed an efficient DNA condensation, facilitated the control of the formulation process preventing the formation of aggregates and contributed to protection against DNAse degradation. These results confirmed and improved previous results using HEK293T cells [16], in which the transfection efficiency of the novel P:DNA:CO-SLN complexes increased more than 200 times, which is remarkable for a non-viral delivery system. The highest transfection activity was obtained at a P:DNA:CO-SLNs ratio of 2:1:7, which was the one that displayed the optimal DNA condensation. Importantly, these P:DNA:CO-SLNplexes did not have a cytotoxic effect in human cells under the studied conditions, and the P:DNA:CO-SLN complexes support cell culture for further testing. All data demonstrate the capacity of this P-improved formulation to carry and deliver nucleic acids into the cytoplasm and nucleus of mammalian cells with high efficiency, making this formulation a promising DNA-carrier for either therapeutic or prophylactic purposes. The results presented herein encourage the use of this novel formulation for further investigations in therapeutic/vaccine research studies. Studies in these fields are currently ongoing by our research work.

Conclusion

The incorporation of protamine into the CO-SLNs allowed to obtain a versatile nanovector that is able to efficiently transfect cells widening the potential applications of SLN-based vectors for gene therapy and/or DNA vaccination. The P:DNA:CO-SLN SLNplexes at a ratio of 2:1:7 was considered the optimal formulation that reached the equilibrium conditioned by the degree of gene protection, the binding ability of P:DNA to CO-SLNs, and the DNA topology for *in vitro* transfection assays. Further *in vivo* experiments are needed to assess the capability of this novel formulation to be used as an effective strategy for gene therapy and/or DNA vaccination.

Conflicts of interest

The authors declare no conflicts of interest.

Acknowledgments

This work was supported by grants from Agencia Nacional de Promoción Científica y Técnica (ANPCyT, Grant PICT 201-0206), the Spanish Ministry of Economy and Competitiveness (grant number BFU2017-89179-R) and the Andalusian Government (Excellence Project BIO-2515/2012) to CS and from the Spanish Ministry of Economy and Competitiveness (grant number BFU2016- 79699-P) to CHM. Support from the European Region Development Fund (ERDF [FEDER]) is also acknowledged. ADN, MLC and GRC are staff members of CONICET. MJL thanks CONICET for her doctoral scholarship.

REFERENCES

1. A. Ghanem, R. Healey and F.G. Adly, Anal. Chim. Acta, 760 (2013) 1-15, doi: 10.1016/j.aca.2012.11.006.

2. P.S. Apaolaza, D. Delgado, A. del Pozo-Rodríguez, A.R. Gascón and M.A. Solinís. Int. J. Pharm., 465 (2014) 413-26, doi: 10.1016/j.ijpharm.2014.02.038.

3. M. Foldvari, D.W. Chen, N. Nafissi, D. Calderon, L. Narsineni and A. Rafiee. J. Control. Release., 240 (2016) 165-90, doi: 10.1016/j.jconrel.2015.12.012.

4. J.C.M. van der Loo and J.F. Wright. Hum. Mol. Genet., 25 (2016) R42–R52, doi: 10.1093/hmg/ddv451.

5. M. Ramamoorth and A. Narvekar. J. Clin. Diagn. Res., 9 (2015) GE01-6, doi: 10.7860/JCDR/2015/10443.5394.

6. C. Carrillo, J.M. Suñé, P. Pérez-Lozano, E. García-Montoya, R. Sarrate, A. Fàbregas, M. Miñarro and J.R. Ticó. Biomed. Pharmacother., 68 (2014) 775-83, doi: 10.1016/j.biopha.2014.07.009.

7. A. del Pozo-Rodríguez, D. Delgado, M.A. Solinís, A.R. Gascón and J.L. Pedraz. Int. J. Pharm., 339 (2007) 261-8, doi: 10.1016/j.ijpharm.2007.03.015.

8. S. Mansouri, P. Lavigne, K. Corsi, M. Benderdour, E. Beaumont and J.C. Fernandes. Eur. J. Pharm. Biopharm., 57 (2004) 1-8, doi: 10.1016/S0939-6411(03)00155-3.

9. S. Mukherjee, S. Ray and R.S. Thakur. Indian J. Pharm. Sci., 71 (2009) 349-58, doi: 10.4103/0250-474X.57282.

10. R.H. Müller, K. Mäder and S. Gohla. Eur. J. Pharm. Biopharm., 50 (2000) 161-77, doi: 10.1016/S0939-6411(00)00087-4.

11. S. Weber, A. Zimmer and J. Pardeike. Eur. J. Pharm. Biopharm., 86 (2014) 7–22, doi: 10.1016/j.ejpb.2013.08.013.

12. M.B. De Jesus and I.S. Zuhorn. J. Control Release, 201 (2015) 1–13, doi: 10.1016/j.jconrel.2015.01.010.

13. B. Zhao, S. Gu, Y. Du, M. Shen, X. Liu and Y. Shen. Int. J. Pharm., 535 (2018) 164–71, doi: 10.1016/j.ijpharm.2017.10.040.

14. C. Botto, N. Mauro, E. Amore, E. Martorana, G. Giammona, M.L. BondÌ. Int. J. Pharm., 516 (2017) 334-41, doi: 10.1016/j.ijpharm.2016.11.052.

15. A. Fàbregas, S. Prieto-Sánchez, M. Suñé-Pou, S. Boyero-Corral, J.R. Ticó, E. García-Montoya, P. Pérez-Lozano, M. Miñarro, J.M. Suñé-Negre, C. Hernández-Munain and C. Suñé. Int. J. Pharm., 516 (2017) 39-44, doi: 10.1016/j.ijpharm.2016.11.026.

16. M. Suñé-Pou, S. Prieto-Sánchez, Y. El Yousfi, S. Boyero-Corral, A. Nardi-Ricart, I. Nofrerias-Roig, P. Pérez-Lozano, E. García-Montoya, M. Miñarro-Carmona, J.R. Ticó, J.M. Suñé-Negre, C. Hernández-Munain and C. Suñé. Int. J. Nanomedicine, 13 (2018) 3223-33, doi: 10.2147/IJN.S158884.

17. P.S. Apaolaza, A. Del Pozo-Rodríguez, M.A. Solinís, J.M. Rodríguez, U. Friedrich, J. Torrecilla, B.H.F. Weber and A. Rodríguez-Gascón. Biomaterials, 90 (2016) 40-9, doi: 10.1016/j.biomaterials.2016.03.004.

18. Y. Byun, V.K. Singh and V.C. Yang. Thromb. Res., 94 (1999) 53-61, doi: 10.1016/S0049-3848(98)00201-1.

19. J.H. Levy, J.R. Zaidan and B. Faraj. Anesth. Analg., 65 (1986) 739-42.

20. J. Maurer, S. Haselbach, O. Klein, D. Baykut, V. Vogel and W. Mäntele. J. Am. Chem. Soc., 133 (2011) 1134-40, doi: 10.1021/ja109699s.

21. F.L. Sorgi, S. Bhattacharya and L. Huang. Gene Ther., 4 (1997) 961-8, doi:10.1038/sj.gt.3300484.

22. P. Li, S. Chen, Y. Jiang, J. Jiang, Z. Zhang and X. Sun. Nanotechnology, 24 (2013) 295101, doi: 10.1088/0957-4484/24/29/295101.

23. Y. Hu, R. Singh, Z. Deng, A. Mintz and W. Hsu. J. Biomed. Nanotechnol., 12 (2016) 1952-61, doi: 10.1166/jbn.2016.2236.

24. V. Rengaswamy, D. Zimmer, R. Süss and J. Rössler. J Control. Release, 235 (2016) 319-27, doi: 10.1016/j.jconrel.2016.05.063.

25. D. Delgado, A. del Pozo-Rodríguez, M.A. Solinís and A. Rodríguez-Gascón. Eur. J. Pharm. Biopharm., 79 (2011) 495-502, doi: 10.1016/j.ejpb.2011.06.005.

26. D. Delgado, A. del Pozo-Rodríguez, M.A. Solinís, M. Avilés-Triqueros, B.H.F. Weber, E. Fernández and A.R. Gascón. Hum. Gene Ther., 23 (2012) 345-55, doi: 10.1089/hum.2011.115.

27. A. Fàbregas, N. Sánchez-Hernández, J.R. Ticó, E. García-Montoya, P. Pérez-Lozano, J.M. Suñé-Negre, C. Hernández-Munain, C. Suñé and M. Miñarro. Int. J. Pharm., 473 (2014) 270-9, doi: 10.1016/j.ijpharm.2014.06.022.

28. E. Vighi, M. Montanari, B. Ruozi, G. Tosi, A. Magli and E. Leo. Eur. J. Pharm. Biopharm., 76 (2010) 384-93, doi: 10.1016/j.ejpb.2010.07.012.

29. P. Greenspan, E.P. Mayer and S.D. Fowler. J. Cell. Biol., 100 (1985) 965-73, doi: 10.1083/jcb.100.3.965.

30. M. Sánchez-Álvarez, A.C. Goldstrohm, M.A. Garcia-Blanco and C. Suñé. Mol. Cell. Biol., 26 (2006) 4998–5014, doi: 10.1128/MCB.01991-05.

31. M. Suñé-Pou, M.J. Limeres, I. Nofrerias, A. Nardi-Ricart, S. Prieto-Sánchez, Y. El-Yousfi, P. Pérez-Lozano, E. García-Montoya, M. Miñarro-Carmona, J.R. Ticó, C. Hernández-Munain, C. Suñé and J.M. Suñé-Negre. Colloids Surf. B: Biointerfaces, 180 (2019) 159-67, doi: 10.1016/j.colsurfb.2019.04.037.

32. K. Wrobel, E. Claudio, F. Segade, S. Ramos and P.S. Laze. J. Immunol. Methods, 189 (1996) 243–9.

33. T. Kanazawa, Y. Takashima, M. Murakoshi, Y. Nakai, H. Okada. Int. J. Pharm., 379 (2009) 187–195, doi: 10.1016/j.ijpharm.2009.06.015.

34. M. Hoare, U. Greiser, S. Schu, K. Mashayekhi, E. Aydogan, M. Murphy, F. Barry, T. Rittler and T. O'Brien. J. Gene Med., 12 (2010) 207–18, doi: 10.1002/jgm.1426.

35. Y. Shen, H. Peng, S. Pan, M. Feng, Y. Wen, J. Deng, X. Luo and C. Wu. Nanotechnology, 21 (2010) 045102–13, doi: 10.1088/0957-4484/21/4/045102.

36. J. Liu, S. Guo, Z. LI, J. Gu. Colloids Surf. B: Biointerfaces, 73 (2009) 36–41, doi: 10.1016/j.colsurfb.2009.04.026.

37. H. Faneca, S. Simões and M.C. Pedroso de Lima. Biochim. Biophys. Acta, 1567 (2002) 23-33, doi: 10.1016/S0005-2736(02)00545-X.

38. J.M. Priegue, I. Lostalé-Seijo, D. Crisan, J.R. Granja, F. Fernández-Trillo and J. Montenegro. Biomacromolecules, 19 (2018) 2638–49, doi: 10.1021/acs.biomac.8b00252.

39. C. Olbrich, U. Bakowsky, C.M. Lehr, R.H. Müller and C. Kneuer. J. Control. Release, 77 (2001) 345–55, doi: 10.1016/S0168-3659(01)00506-5.

40. C. Tros de Ilarduza, Y. Sun and N. Düzgüneş. Eur. J. Phar. Sci., 40 (2010) 159-70, doi: 10.1016/j.ejps.2010.03.019.

41. E. Lepeltier, L. Nuhn, C.M. Lehr and R. Zentel. Nanomedicine (Lond.), 10 (2015) 3147-66, doi: 10.2217/nnm.15.132.

42. S.M. Dizaj, S. Jafari and A.Y. Khosroushahi. Nanoscale Res. Lett., 9 (2014) 252, doi: 10.1186/1556-276X-9-252.

43. K. Remaut, N.N. Sanders, F. Fayazpour, J. Demeester and S.C. De Smedt. J Control. Release, 115 (2006) 335-43, doi: 10.1016/j.jconrel.2006.08.009.

44. N.N. Sanders, S.C. J. De Smedt and J. Demeester, Therapeutic enzymes, in: B.M. McGrath, G. Walsh (Eds), Directory of therapeutic enzymes, Taylor & Francis Group, Boca Raton, 2006, pp. 97-116.

45. F.L. Sorgi, S. Bhattacharya and L. Huang. Gene Ther., 4 (1997) 961-8, doi: 10.1038/sj.gt.3300484.

46. J. Ye, A. Wang, C. Liu, Z. Chen and N. Zhang. Nanotechnology, 19 (2008) 285708, doi: 10.1088/0957-4484/19/28/285708.